Author Manuscript

Author Manuscript

Author Manuscript

Author Manuscript

HHS Public Access

Author manuscript

Oncogene. Author manuscript; available in PMC 2016 November 12.

Published in final edited form as:

Oncogene. 2016 November 3; 35(44): 5713–5721. doi:10.1038/onc.2016.111.

Distinct downstream targets manifest p53-dependent pathologies in mice

V Pant[1], **S Xiong**[1], **G Chau**[1], **K Tsai**[2], **G Shetty**[3], and **G Lozano**[1]

[1]Department of Genetics, The University of Texas, MD Anderson Cancer Center, Houston, TX, USA

[2]Department of Dermatology, The University of Texas, MD Anderson Cancer Center, Houston, TX, USA

[3]Department of Experimental Radiation Oncology, The University of Texas, MD Anderson Cancer Center, Houston, TX, USA

Abstract

Mdm2, the principal negative regulator of p53, is critical for survival, a fact clearly demonstrated by the p53-dependent death of germline or conditional mice following deletion of *Mdm2*. On the other hand, *Mdm2* hypomorphic ($Mdm2^{Puro/\Delta 7-12}$) or heterozygous ($Mdm2^{+/-}$) mice that express either 30 or 50% of normal Mdm2 levels, respectively, are viable but present distinct phenotypes because of increased p53 activity. Mdm2 levels are also transcriptionally regulated by p53. We evaluated the significance of this reciprocal relationship in a new hypomorphic mouse model inheriting an aberrant *Mdm2* allele with insertion of the neomycin cassette and deletion of 184-bp sequence in intron 3. These mice also carry mutations in the *Mdm2* P2-promoter and thus express suboptimal levels of Mdm2 entirely encoded from the P1-promoter. Resulting mice exhibit abnormalities in skin pigmentation and reproductive tissue architecture, and are subfertile. Notably, all these phenotypes are rescued on a *p53*-null background. Furthermore, these phenotypes depend on distinct p53 downstream activities as genetic ablation of the pro-apoptotic gene *Puma* reverts the reproductive abnormalities but not skin hyperpigmentation, whereas deletion of cell cycle arrest gene *p21* does not rescue either phenotype. Moreover, p53-mediated upregulation of *Kitl* influences skin pigmentation. Altogether, these data emphasize tissue-specific p53 activities that regulate cell fate.

INTRODUCTION

Mdm2, the principal negative regulator of p53, inhibits its stability and activity. Regulation of p53 activity by Mdm2 is critical for survival, a fact clearly demonstrated by p53-dependent early embryonic lethality of *Mdm2*-null mice.[1,2] Also, conditional deletion of

Correspondence: Dr G Lozano, Department of Genetics, The University of Texas, MD Anderson Cancer Center, 1515 Holcombe Boulevard, Houston, TX 77030, USA. gglozano@mdanderson.org.

CONFLICT OF INTEREST

The authors declare no conflict of interest.

Supplementary Information accompanies this paper on the Oncogene website (http://www.nature.com/onc)

Author Manuscript Author Manuscript Author Manuscript Author Manuscript

Mdm2 in most major tissues of adult mice imparts lethality.[3–6] On the other hand, normal viability and survival of $Mdm2^{+/-}$ mice suggests that 50% Mdm2 levels are sufficient to adequately regulate p53.[7] A further reduction in Mdm2 levels to ~30% imparts a distinct phenotype in mice including lymphopenia, small size and radiation sensitivity.[8] Interestingly, Mdm2 is itself a transcriptional target of p53 and is transcribed from two different promoters (P1 and P2).[9] Both RNA transcripts encode the same full-length Mdm2 protein.[10,11] The P1-promoter is constitutive and accounts for the baseline Mdm2 levels necessary for regulating p53 in a cell. The P2-promoter on the other hand is p53-dependent and transcribed in response to stress-induced p53 binding at the internally located response elements.[12] Thus, p53 and Mdm2 share an intimate autoregulatory relationship wherein p53 promotes the expression of Mdm2, which in turn inhibits p53 stability and activity. We recently examined this relationship in a genetically engineered mouse model wherein binding of p53 at the *Mdm2* P2-promoter and its resultant activation were abrogated.[13] Mice that lacked p53-mediated activation of P2-*Mdm2* were normal in all aspects, and lived a normal life span but were extremely radiosensitive and succumbed to bone marrow aplasia following exposure to sublethal 6 Gy irradiation (IR). These results indicated that p53-Mdm2 autoregulation is critical only under DNA damage conditions and is dispensable for normal development and survival. Moreover, basal levels of Mdm2 (from P1-promoter) are sufficient to regulate p53 under homeostatic conditions.

Fortuitously, while generating these mice, we also generated an aberrant allele ($Mdm2^{PND}$) in which one of the *loxP* sites flanking the neomycin cassette was lost along with a 184-bp sequence from intron 3. Intriguingly, homozygous mice had a distinct dark coloration that drew our attention.

We thus carried out a detailed characterization of homozygous $Mdm2^{PND/PND}$ mice and show that they have suboptimal levels of Mdm2 encoded entirely by the P1-promoter. This results in augmentation of specific p53 activity, which manifests distinct phenotypic abnormalities in mice. $Mdm2^{PND/PND}$ mice exhibit abnormal accumulation of melanocytes in the extremities. In addition, they show defects in the hematopoietic system and atrophy of gonads. These p53-dependent phenotypes depend on activation of distinct tissue-specific p53 transcriptional targets as genetic ablation of *Puma* rescues the hematopoietic and reproductive tissue defects but not skin hyperpigmentation, whereas loss of *p21* does not rescue either of these defects. Moreover, *kitl*, another p53 transcriptional target is solely responsible for skin hyperpigmentation. These data highlight the multifaceted role of the p53 tumor suppressor in development and its functionality in hematopoiesis, reproduction and skin pigmentation.

RESULTS

Characterization of $Mdm2^{PND/PND}$ mice

$Mdm2^{PND/PND}$ mice were obtained during the generation of the $Mdm2^{P2/P2}$ allele. The strategy for generating $Mdm2^{P2/P2}$ mice has been described previously.[13] Following germline transmission, the alleles were characterized and the *Mdm2* locus sequenced to ensure accuracy of recombination. In one mouse, sequencing results revealed deletion of a *loxP* site flanking the neomycin selection cassette along with 184 bp of DNA from intron 3

Author Manuscript Author Manuscript Author Manuscript Author Manuscript

(Figure 1a, Supplementary Figure 1). Consequently, the neomycin cassette could not be excised out by Cre-mediated recombination. This resulted in a novel *Mdm2* allele that carries a mutant P2-promoter with alterations in the p53-binding sites, a neomycin gene, and a 184-bp deletion in intron 3 and is henceforth called $Mdm2^{PND}$.

To analyze whether this inadvertent recombination event resulted in a functional *Mdm2* allele, we intercrossed heterozygous $Mdm2^{PND/+}$ mice to generate homozygous $Mdm2^{PND/PND}$ mice, which were viable. As ablation of Mdm2 expression is incompatible with life, the viability of homozygous $Mdm2^{PND/PND}$ mice confirmed that functional Mdm2 was indeed being expressed in these mice. Next, to examine whether Mdm2 P2-promoter function, which is DNA damage responsive, was indeed abrogated in $Mdm2^{PND/PND}$ mice because of the intended mutations at the p53 response elements, we performed reverse transcriptase (RT)–quantitative PCR (qPCR) for *Mdm2* in RNA isolated from thymi of un-irradiated and irradiated wild-type and homozygous $Mdm2^{PND/PND}$ mice (Figure 1b). As expected, *Mdm2* mRNA was induced only in irradiated wild-type mouse thymus while no induction of *Mdm2* RNA was observed in un-irradiated $Mdm2^{PND/PND}$ samples. To further examine the effect of low Mdm2 levels on p53 transactivation function on other canonical targets, we performed RT–qPCR for *p21* and *Puma* in irradiated thymic RNA samples (Figure 1b). Both of these targets were substantially upregulated in irradiated $Mdm2^{PND/PND}$ thymi implying normal damage-responsive p53 activity in $Mdm2^{PND/PND}$. Of note, *p21* induction was significantly higher in irradiated $Mdm2^{PND/PND}$ thymic RNA for unknown reasons. These data confirmed the novelty of $Mdm2^{PND}$ allele.

The DNA damage studies described above also indicated that basal levels of *p21* and *Puma* were significantly elevated in un-irradiated $Mdm2^{PND/PND}$ thymic RNA samples (Figure 1b). We thus expanded these studies to include analyses of basal *p21* and *Puma* levels in spleens, another tissue known to be sensitive to minor changes in p53 levels, and testes as preliminary dissection of mice (see below) indicated reproductive defects. Comparative RT–qPCR analysis for *p21* and *Puma* as surrogates for p53 function revealed elevated basal p53 activity in spleens and testis of these mice as compared with the wild-type controls (Figure 1c and Supplementary Figure 1). Finally, since the functional role of Mdm2 as the principal E3-ligase for p53 is dependent on its protein levels,[14,15] we next examined basal levels of Mdm2 protein in homozygous $Mdm2^{PND/PND}$ mice. Immunoblotting revealed very low levels of Mdm2 protein in testes lysate from $Mdm2^{PND/PND}$ mice (Figure 1d). Similarly, a reciprocal increase in p53 levels was also observed. This suggests that these mice express suboptimal levels of Mdm2 protein solely from the transcript originating from the P1-promoter that is insufficient to regulate basal levels of p53 in several tissues. In agreement with increased p53 activity, we also observed increased apoptosis in thymi and testes of $Mdm2^{PND/PND}$ mice by terminal deoxynucleotidyl transferase-mediated dUTP nick end labeling (TUNEL) staining (Figure 1e).

To ascertain Mdm2 levels and to test genetically whether Mdm2 levels can be further reduced in these mice, we set up a cross between $Mdm2^{PND/PND}$ and $Mdm2^{+/-}$ mice. Despite repeated breeding attempts, we could not generate $Mdm2^{PND/-}$ mice (0/25; 50% frequency expected). This indicates that homozygous $Mdm2^{PND/PND}$ mice express Mdm2 close to the threshold level for survival.

Author Manuscript Author Manuscript Author Manuscript Author Manuscript

Mdm2^{PND} mice are physically normal but exhibit hyperpigmented skin

Previous studies have shown that decreased Mdm2 levels affect body size in mice.[8] To examine whether a similar phenotype is evident in *Mdm2*$^{PND/PND}$ mice, we compared the size, and weight of *Mdm2*$^{PND/PND}$ and wild-type mice. Young (6 weeks old) homozygous male and female *Mdm2*$^{PND/PND}$ homozygous mice were indistinguishable from wild-type mice in size and slight differences in weight were not statistically significant (Figure 2a). However, the difference in weight was significant (P=0.009) in older mice (1-year old). Moreover, homozygous *Mdm2*$^{PND/PND}$ mice had a distinctly dark skin especially obvious in the tail, feet and ears (Figure 2b). Increase in skin pigmentation was first noticeable in postnatal day 4 (P4) *Mdm2*$^{PND/PND}$ mouse pups and the intensity progressed with age. Separation of skin into epidermal and dermal layers revealed that the hyperpigmentation was restricted to the epidermal layer and the dermis was not affected (Figure 2c). Histopathology analyses of skin samples revealed that *Mdm2*$^{PND/PND}$ mice had extensive accumulation of melanocytes in the basal layer of interfollicular epidermis and also had increased numbers of spindled melanocytes, a phenomenon not typically observed in normal wild-type mouse skin (Figure 2d). Fontanna masson staining further confirmed markedly higher melanin content in *Mdm2*$^{PND/PND}$ mouse tail sections (Figure 2d). Previously published literature has documented similar hyper-pigmented skin phenotype in knock out mouse models of ribosomal genes and to a lesser degree in heterozygous *Mdm2* mice because of increased p53 activity.[16–18]

Mdm2$^{PND/PND}$ mice have defects in reproductive organs and reduced fertility

To examine whether in addition to the dark skin phenotype *Mdm2*$^{PND/PND}$ mice also harbor additional abnormalities, we performed complete morphologic and histologic analysis of major murine tissues. The size and weight of brain, spleen and thymus from 6 weeks old *Mdm2*$^{PND/PND}$ mice was comparable to similar aged wild-type mouse organs (Supplementary Figures 2A and B). Histologic evaluation of these samples also did not reveal any significant differences. However, the heart (P=0.02) and the reproductive organs (P=0.013) of *Mdm2*$^{PND/PND}$ mice were significantly smaller (Figures 3a and b). Interestingly, the difference in heart weight was not significant in older (1 year) mice. Moreover, histologic evaluation of heart in 6 weeks and 1-year old mice showed normal morphological features. On the other hand, microscopic examination of testes and ovaries from *Mdm2*$^{PND/PND}$ mice presented distinct changes in architecture (Figure 3c). In the *Mdm2*$^{PND/PND}$ mouse testis, the percentage of seminiferous tubules with germ cells was significantly reduced from 100 to 66%. Furthermore, only 59% of these tubules carried differentiated germ cells (showing germ cells at the stage of at least B spermatogonia with or without the advanced stages of spermatocytes and spermatids) (Figure 3d). The percentage of tubules containing round and condensed spermatids were reduced to 7% in these mice compared with 100% in controls, suggesting additional impairment at the meiotic process. As noted above, an increase in apoptotic germ cells was clearly evident in *Mdm2*$^{PND/PND}$ mouse testes by TUNEL staining (Figure 1e). Similarly, in the female germline there was an apparent reduction in the size of uterine horns of *Mdm2*$^{PND/PND}$ mice (Figure 3a). Moreover, representative sections of *Mdm2*$^{PND/PND}$ mouse ovaries showed a reduction in the number of growing secondary, preantral and antral follicles compared with the wild-type controls along with an apparent increase in the number of atretic follicles (Figure 3c).

Author Manuscript Author Manuscript Author Manuscript Author Manuscript

Despite the obvious differences in reproductive organ size, and inefficient mature germ cell development, some homozygous *Mdm2*$^{PND/PND}$ mice of both sexes were fertile, although subtle differences were noted. *Mdm2*$^{PND/PND}$ females mated to wild-type mice produced a limited number of progeny and females older than 3 months had problems breeding. These subfertile defects were compounded upon intercrossing of homozygous *Mdm2*$^{PND/PND}$ mice. During the monitoring period of 7 months, a typical male and female pair of *Mdm2*$^{PND/PND}$ homozygous mice yielded a maximum of 2 litters with an average litter size of 5 pups in contrast to >5 litters of 8–10 pups by a wild-type breeding pair. In addition, the number of homozygous *Mdm2*$^{PND/PND}$ female mice recovered at weaning was limited (19/95, $P < 0.0001$) suggesting possible sensitivity of female embryos to decreased Mdm2 levels. Altogether, these data highlight the sensitivity of the reproductive tissues, particularly the germ cells to decreased Mdm2 levels.

Mdm2$^{PND/PND}$ mice display hematopoietic defects and are extremely radiosensitive

Reduced levels of Mdm2 are implicated in the hematopoietic defects observed in *Mdm2* hypomorphic mice.[8] To examine whether similar defects are also emphasized in *Mdm2*$^{PND/PND}$ mice, we performed complete blood cell count analysis of these mice. Indeed, *Mdm2*$^{PND/PND}$ mice exhibited mild anemia and leucopenia in comparison with age/sex and background matched wild-type mice (Figure 4a).

Changes in Mdm2 levels in mice also impart characteristic radiosensitivity in mice.[7,8,13,19,20] In agreement with this, *Mdm2*$^{PND/PND}$ mice succumbed to death following exposure to 6 Gy IR, a dose that does not affect short-term survival of wild-type mice (data not shown).[13] Further titration of the radiation dosage indicated that *Mdm2*$^{PND/PND}$ mice remained hypersensitive to even a milder 3 Gy IR exposure and succumbed to radiation afflicted bone marrow aplasia (Figure 4b and data not shown). This further affirms the increase in unregulated p53 activity in *Mdm2*$^{PND/PND}$ mice after IR. Together, these data support the necessity of p53 regulation in development and maintenance of the hematopoietic system.

Mdm2$^{PND/PND}$ mouse phenotypes are p53 dependent

To test whether skin hyperpigmentation, reproductive tissue atrophy and other associated changes in homozygous *Mdm2*$^{PND/PND}$ were p53-dependent phenotypes, we crossed *Mdm2*$^{PND/PND}$ mice onto a *p53*-null background. Absence of a single *p53* allele restored the normal size of heart and testes in *Mdm2*$^{PND/PND}$ *p53*$^{+/-}$ mice (Figure 5a). Furthermore, the deficiencies of spermatogenesis and ovarian follicular development in *Mdm2*$^{PND/PND}$ mouse were completely alleviated in *p53*$^{+/-}$ background (Figures 5b and c). More importantly, loss of a single p53 allele reduced the hyperpigmentation of skin, ears, paws and tail (data not shown). Complete biallelic loss of *p53* entirely restored the normal skin tone in *Mdm2*$^{PND/PND}$ *p53*$^{-/-}$ mice (Figure 5d). In addition, loss of p53 also rescued the radiation hypersensitivity of *Mdm2*$^{PND/PND}$ mice to 3 Gy IR (data not shown).

Mdm2$^{PND/PND}$ mouse phenotypes depend on distinct p53 downstream activities

Although p53 has been implicated in atrophy of reproductive organs and skin pigmentation,[16,21] the importance of downstream p53 targets involved in manifestation of

Author Manuscript Author Manuscript Author Manuscript Author Manuscript

these phenotypes has not been well defined. Major p53 activities are coupled with its ability to transactivate downstream cell cycle arrest and apoptosis genes. To closely examine the involvement of p53 cell cycle arrest and apoptosis functions in reproductive tissue atrophy and skin hyperpigmentation, we crossed *Mdm2*$^{PND/PND}$ mice to *p21*-null or *Puma*-null mice. Although loss of *p21* partially alleviated the testes size (Figure 5a), it did not revert spermatogenesis or fertility defects of *Mdm2*$^{PND/PND}$ mice (Figures 5b and c and data not shown). In fact, loss of *p21* exacerbated the tissue atrophy phenotype. Of note, *Mdm2*$^{PND/PND}$ *p21*$^{-/-}$ female mice were not recovered, which suggests further sensitization of female embryos to defects. In contrast, complete loss of *Puma* fully rescued the reproductive tissue defects of *Mdm2*$^{PND/PND}$ mice (Figures 5b and c). Cross-section of testes and ovaries from *Mdm2*$^{PND/PND}$ *Puma*$^{-/-}$ mice showed normal histomorphology and intercrossing of these mice yielded normal litter size and numbers (Figures 5b and c and data not shown).

Next, we evaluated the role of *p21* and *Puma* in skin hyperpigmentation phenotype of *Mdm2*$^{PND/PND}$ mice. Interestingly, absence of either *p21* or *Puma* alone did not alter the skin hyperpigmentation phenotype. In fact, even the combined absence of *p21* and *Puma* did not alter the skin phenotype in *Mdm2*$^{PND/PND}$ mice. *Mdm2*$^{PND/PND}$ *p21*$^{-/-}$, *Mdm2*$^{PND/PND}$ *Puma*$^{-/-}$ and *Mdm2*$^{PND/PND}$ *p21*$^{-/-}$ *Puma*$^{-/-}$ mice still exhibited hyperpigmented skin phenotype in the extremities (Figure 5d and data not shown).

p53 is essential for accumulation and maintenance of melanocytes in mouse skin

As noted above, skin hyperpigmentation is a p53-dependent phenotype caused by improper accumulation of melanocytes in the epidermis. Previous studies have identified kit ligand (Kitl) as a p53 transcriptional target that is involved in melanocyte migration.[16,22] Transgenic mice that express Kitl under the K14 promoter exhibit a similar skin hyperpigmentation phenotype.[23] To evaluate whether excessive p53-dependent Kitl expression is associated with hyperpigmentation of *Mdm2*$^{PND/PND}$ extremities, we performed RT–qPCR for *Kitl* in keratinocyte RNA from these mice. Indeed, *Kitl* expression was significantly higher in *Mdm2*$^{PND/PND}$ mice (P=0.03) compared with wild-type keratinocytes (Figure 6a). Thus, these data point to the involvement of elevated levels of the p53 target *Kitl* in aberrant accumulation of melanocytes causing hyperpigmentation of *Mdm2*$^{PND/PND}$ mice.

Next, we further evaluated the role of p53 in maintenance of aberrantly accumulated melanocytes in mice. Previous studies have shown that injection of anti-kit antibody during the first 4 days of postnatal life impedes melanoblast migration and prevents skin hyperpigmentation in mice, however, it has no effect on melanocytes that have already migrated and accumulated.[16,24,25] Moreover, the role of p53 in maintenance of these accumulated melanocytes in mice is not clear. To address this issue, we generated compound *Mdm2*$^{PND/PND}$ *p53*$^{flox/flox}$*: CreERT2* mice. These mice carried a floxed *p53* allele along with a tamoxifen-sensitive *Cre* transgene and as expected had dark skin pigmentation because of functional p53 activity. Conditional deletion of p53 was carried out by tamoxifen injection in 5–6 weeks old mice. Amazingly, p53 deletion largely alleviated the dark skin pigmentation phenotype in *Mdm2*$^{PND/PND}$ *p53*$^{flox/flox}$*: CreERT2* mice (Figure 6b). Skin

Author Manuscript Author Manuscript Author Manuscript Author Manuscript

sections revealed the disappearance of accumulated melanocytes from the epidermal layer (Figure 6b). This suggests that in addition to affecting melanocyte migration/accumulation, p53 is also involved in maintenance of accumulated melanocytes in mice.

Mdm2$^{PND/PND}$ have a shorter life span

Finally, we examined whether enhanced p53 activation alters life span of *Mdm2*$^{PND/PND}$ mice. We compared the survival of a cohort of wild-type and *Mdm2*$^{PND/PND}$ mice for 2 years. The wild-type survival data was previously published with *Mdm2*$^{P2/P2}$ mice,[13] and is compared here because all mouse cohorts were maintained in the facility at the same time. In comparison with wild-type mice (median survival 778.5 days), more *Mdm2*$^{PND/PND}$ mice (median survival 670.5 days) died during the monitoring time period (P=0.03) (Figure 7). Although we did not explore the cause of death in these mice, a few (3/20) of *Mdm2*$^{PND/PND}$ mice were flagged for tumor burden late in life (over 23 months). Pathology report conveyed fibrosarcoma and lymphoma as the major tumor types. Lymphomas were also observed in some of the aged wild-type mice (3/20). This suggests augmentation of p53 activity beyond a certain threshold negatively affects life span and offers no additional protection against tumorigenesis.

DISCUSSION

Regulation of p53 activity by Mdm2 is important for proper manifestation of tissue morphology and function. Many different mouse models with alterations in p53–Mdm2 relationship have been previously generated and characterized.[26] Here we report the characterization of a new hypomorphic *Mdm2* allele that carries a neomycin gene along with a 184-bp deletion in intron 3. In addition, these mice also have a mutant *Mdm2* P2-promoter that is not responsive to p53. Resulting *Mdm2*$^{PND/PND}$ mice express Mdm2 levels close to the minimal threshold limit, which cannot be reduced further (halved) without sacrificing viability. The corresponding increase in basal p53 activity in *Mdm2*$^{PND/PND}$ mice leads to major morphological and functional anomalies in a subset of tissues. *Mdm2*$^{PND/PND}$ mice exhibit hyperpigmentation in different extremities because of melanocyte accumulation in the basal layer of interfollicular epidermis. Of note, the hyperpigmentation phenotype is not entirely due to the presence of neomycin cassette alone as the correctly targeted *Mdm2*^{P2P2} mice with neomycin selection cassette (before Cre-deletion) do not exhibit similar phenotype.[13] As mentioned earlier, *Mdm2*$^{PND/PND}$ mice also lack a 184-bp sequence in intron 3. Whether this missing sequence carries some important regulatory elements that have a role in p53 regulation is not clear. A cursory examination of potential binding factors did not reveal anything significant. Nonetheless, hyperpigmentation is a p53-dependent phenomenon and not typical of normal mice where melanocyte accumulation is restricted to the follicles.[16,27] The phenotype is reminiscent of similar observations reported in *K14-Kitl* transgenic mice because of increased c-kit signaling in the epidermis.[23,24] In agreement, we observed increase in *Kitl* mRNA levels in keratinocytes of *Mdm2*$^{PND/PND}$ mice. Kitl is an important down-stream target of p53 activity and acts a chemokinetic factor that accelerates melanoblast migration to the hair follicles in the skin of a developing embryo.[27] Thus, in the absence of sufficient Mdm2 necessary for regulating p53 during early development

Author Manuscript Author Manuscript Author Manuscript Author Manuscript

increased p53-mediated upregulation of Kitl affects melanoblast migration and causes aberrant accumulation of melanocytes in the epidermis.

We also identified an important role of p53 in maintenance of accumulated melanocytes in mice. Somatic deletion of p53 in *Mdm2*$^{PND/PND}$ mice restored normal skin pigmentation. Whether the accumulated melanocytes that cause skin hyperpigmentation in these mice undergo p53-independent death (apoptosis) or migrate to other locations following loss of p53 is not clear. Nonetheless, the p53 downstream target Kitl is likely involved. This suggests that besides affecting melanocyte migration/accumulation, p53 is also involved in maintenance of accumulated melanocytes in mice.

Mdm2$^{PND/PND}$ mice also exhibited atrophy of male and female reproductive tissues. A previous report suggests that p53 has an important role in spermatogonial proliferation and regulation of its apoptotic process during early stage of normal spermatogenesis.[28] In addition, p53 was shown to be primarily expressed in spermatocytes[29] and hence suggested to be a potential regulator of meiotic process. Consistent with these reports, the results from our study indicate that in *Mdm2*$^{PND/PND}$ mice, the hyperactive p53 acts at both levels of the spermatogenic process to cause germ cell loss and thus impair spermatogenesis. The complete absence of germ cells in considerable 34% of the seminiferous tubules in these mice suggests that p53 targets the germ cells at the step of spermatogonial proliferation and possibly their differentiation (Figure 3d). Second, the presence of post-meiotic germ cells (spermatids) in only 7% of the tubules, out of the remaining 66% of the tubules that contain germ cells, indicates that p53-mediated germ cell loss likely occurs at the meiotic stage in these mice. Indeed, we observed increased apoptosis of germ cells in *Mdm2*$^{PND/PND}$ mice testes compared with controls (Figure 1e). In females, follicular development appeared to be impaired as a result of increased atresia of follicles, likely due to apoptosis of granulosa cells and/or oocytes. Amazingly, some mice from both sexes were still fertile indicating that the defect was restricted to cell number only and did not alter the functionality of mature sperm or oocyte. Overall, these data suggest that p53 surveillance is critical in the highly proliferative hematopoietic and reproductive tissues. Augmentation of p53 activity in these tissues leads to acellularity and associated functional defects.

Mdm2$^{PND/PND}$ mice exhibited additional defects in hematopoietic lineage, which rendered them overtly sensitive to low dose IR. Even a trivial 3 Gy IR dose was acutely toxic to *Mdm2*$^{PND/PND}$ mice. Furthermore, *Mdm2*$^{PND/PND}$ mice had a shorter life span compared with wild-type mice and just like wild-type mice *Mdm2*$^{PND/PND}$ mice also developed late age tumors. This suggests that augmentation of p53 activity beyond a certain threshold negatively affects life span and offers no additional protection against tumorigenesis.

The impaired spermatogenesis and ovarian folliculogenesis in *Mdm2*$^{PND/PND}$ mice could be completely rescued upon deletion of the p53 downstream target *Puma*, a pro-apoptotic gene, suggesting an important role of apoptosis in maintenance of spermatogenesis and ovarian follicular development. Previously, in another study, we have shown that Puma is important for preserving the cellularity of bone marrow after total body IR.[13] Yet, another p53 target cell cycle arrest gene *p21* has been implicated in recovery of intestinal cellularity following high-dose radiation exposure.[30] Altogether, these studies highlight the significance of tissue-

Author Manuscript Author Manuscript Author Manuscript Author Manuscript

specific p53 activities in pathological presentations. More so, they emphasize the involvement of distinct p53 downstream targets in manifestation of these pathologies.

Some of the phenotypes observed in *Mdm2*$^{PND/PND}$ mice are slightly different from a previously published study with *Mdm2*$^{Puro/\Delta 7-12}$ mice.[8] This could be due to differences in the targeted *Mdm2* locus (insertion of neomycin in intron 3 versus puromycin insertion in intron 6) and/or background mouse strain used in the studies. Another possible reason for differences is that unlike the other study, *Mdm2*$^{PND/PND}$ mice also carry a mutant P2-promoter and lack the associated ability to transcribe *Mdm2* for regulating stress-induced p53. As a result, p53 levels and activity are slightly higher in *Mdm2*$^{PND/PND}$ mouse tissues.

Overall, this report highlights the importance of a p53 threshold necessary for normal tissue functions and shows that distinct tissue-specific p53 transcriptional targets are involved in the manifestation of p53-dependent pathologies in mice. In addition, a new role of p53 in maintenance of melanocyte accumulation is also uncovered. These data emphasize the growing repertoire of tissue-specific p53 activities that require further mechanistic characterization.

MATERIALS AND METHODS

Mouse maintenance and genotyping

Mice were maintained in >90% C57Bl/6 background and all studies were conducted according to IACUC approved protocol. Mouse genotyping was carried out as previously described.[13,31] *Puma*-null mice were kindly provided by G Zambetti.[32] *p53-null*,[33] *p21-null*,[34] *Cre-ERT2*[35] (Tamoxifen inducible Cre transgene in *ROSA26* locus) and *p53*$^{flox/flox}$ mice[36] were purchased from Jackson Laboratory (Bar Harbor, ME, USA).

RNA isolation and RT–qPCR

Total RNA was isolated from tissues using TRIzol reagent (Invitrogen, Carlsbad, CA, USA). One microgram of RNA was reverse transcribed using first-strand synthesis kit (GE Healthcare, Pittsburgh, PA, USA). Reaction was diluted 15-fold and 2 μl of the diluted sample was used in qPCR for p53 targets in 7900HT (Applied Biosystems, Foster City, CA, USA) real-time PCR machine as previously described.[13] Student's *t*-test was performed to examine statistical significance. $P < 0.05$ was considered significant.

Western blotting

Tissue samples were homogenized in NP-40 lysis buffer (50 nM Tris-HCl pH 8.0, 100 mM Nacl, 0.5% NP-40) supplemented with 1× complete protease inhibitor (Roche, Indianapolis, IN, USA). In all, 100 μl of protein lysate was resolved on 8% sodium dodecyl sulfate–polyacrylamide gel electrophoresis. After transfer on nitrocellulose membranes, blots were probed with p53 (CM5, 1:1000, Novacastra, Buffalo Grove, IL, USA), Mdm2 (2A10, 1:500, Calbiochem, San Diego, CA, USA) and Vinculin (V9131, 1:5000, Sigma, St Louis, MO, USA) antibodies.

Author Manuscript Author Manuscript Author Manuscript Author Manuscript

Tissue analyses

Fresh tissues were isolated from mice and recorded for weight. Tissues were fixed in either 10% buffered formalin or Bouin's fixative, embedded in paraffin and sections cut at 7 μm. In testicular sections, tubule differentiation index, percentage of seminiferous tubules containing differentiated germ cells, was determined in periodic acid–Schiff-hematoxylin sections of testis by microscopy as previously described.[37] For analysis of ovarian sections, periodic acid–Schiff-hematoxylin or hematoxylin and eosin-stained sections were used. Hematoxylin and eosin-stained sections of mouse dorsal skin, tail and paws were analyzed for melanocyte accumulation. TUNEL staining was performed using FragEL DNA fragmentation detection kit (Calbiochem) following the manufacturer protocol. For epidermal–dermal separation, mouse tail piece was incubated in 2 M sodium bromide solution at 37 °C for 2 h and skin layers were separated manually using forceps. Hematoxylin and eosin, Fontanna Masson staining and complete blood cell count analyses on peripheral blood was done by veterinary medicine core lab at M.D. Anderson Cancer Center (Houston, TX, USA).

Tamoxifen injection

Five- to 6-week-old mice were intraperitoneally injected with tamoxifen (Sigma, 3 mg/40 g) reconstituted in corn oil. Mice were injected once every 3 days for a total of three times. Pigmentation change was noticed 10 days after the final injection.

Radiation

Six- to 8-week-old mice were irradiated with 3 or 6 Gy in a Cesium-137 irradiator and monitored for survival.

Statistical analyses

Statistical analysis was carried out using GraphPad Prism 6 (Graphpad Software Inc, La Jolla, CA, USA) and shown as mean ± s.e.m. Student's *t*-test was used to confirm statistical significance and *P*-value ≤ 0.05 was considered significant. $*P < 0.05$, $**P < 0.01$, $***P < 0.001$, $****P < 0.0001$. Minimal of three or more biological replicates were used for each experiment. Survival curves were graphed using Kaplan–Meier method and statistical significance calculated by log-rank Mantel–Cox test.

Supplementary Material

Refer to Web version on PubMed Central for supplementary material.

Acknowledgments

Mdm2$^{PND/PND}$ mice were made by the GEM Facility at the MDACC funded by an NCI Cancer Center Support Grant (CA16672). The studies were supported by NIH grant CA47296 to GL.

REFERENCES

1. Jones SN, Roe AE, Donehower LA, Bradley A. Rescue of embryonic lethality in Mdm2-deficient mice by absence of p53. Nature. 1995; 378:206–208. [PubMed: 7477327]

Author Manuscript Author Manuscript Author Manuscript Author Manuscript

2. Montes de Oca Luna R, Wagner DS, Lozano G. Rescue of early embryonic lethality in mdm2-deficient mice by deletion of p53. Nature. 1995; 378:203–206. [PubMed: 7477326]

3. Francoz S, Froment P, Bogaerts S, De Clercq S, Maetens M, Doumont G, et al. Mdm4 and Mdm2 cooperate to inhibit p53 activity in proliferating and quiescent cells *in vivo*. Proc Natl Acad Sci USA. 2006; 103:3232–3237. [PubMed: 16492744]

4. Grier JD, Xiong S, Elizondo-Fraire AC, Parant JM, Lozano G. Tissue-specific differences of p53 inhibition by Mdm2 and Mdm4. Mol Cell Biol. 2006; 26:192–198. [PubMed: 16354690]

5. Xiong S, Van Pelt CS, Elizondo-Fraire AC, Liu G, Lozano G. Synergistic roles of Mdm2 and Mdm4 for p53 inhibition in central nervous system development. Proc Natl Acad Sci USA. 2006; 103:3226–3231. [PubMed: 16492743]

6. Zhang Y, Xiong S, Li Q, Hu S, Tashakori M, Van Pelt C, et al. Tissue-specific and age-dependent effects of global Mdm2 loss. J Pathol. 2014; 233:380–391. [PubMed: 24789767]

7. Terzian T, Wang Y, Van Pelt CS, Box NF, Travis EL, Lozano G. Haploinsufficiency of Mdm2 and Mdm4 in tumorigenesis and development. Mol Cell Biol. 2007; 27:5479–5485. [PubMed: 17526734]

8. Mendrysa SM, McElwee MK, Michalowski J, O'Leary KA, Young KM, Perry ME. Mdm2 Is critical for inhibition of p53 during lymphopoiesis and the response to ionizing irradiation. Mol Cell Biol. 2003; 23:462–472. [PubMed: 12509446]

9. Barak Y, Juven T, Haffner R, Oren M. Mdm2 expression is induced by wild type p53 activity. EMBO J. 1993; 12:461–468. [PubMed: 8440237]

10. Barak Y, Lupo A, Zauberman A, Juven T, Aloni-Grinstein R, Gottlieb E, et al. Targets for transcriptional activation by wild-type p53: endogenous retroviral LTR, immunoglobulin-like promoter, and an internal promoter of the mdm2 gene. Cold Spring Harb Symp Quant Biol. 1994; 59:225–235. [PubMed: 7587074]

11. Wu X, Bayle JH, Olson D, Levine AJ. The p53-mdm-2 autoregulatory feedback loop. Genes Dev. 1993; 7:1126–1132. [PubMed: 8319905]

12. Mendrysa SM, Perry ME. The p53 tumor suppressor protein does not regulate expression of its own inhibitor, MDM2, except under conditions of stress. Mol Cell Biol. 2000; 20:2023–2030. [PubMed: 10688649]

13. Pant V, Xiong S, Jackson JG, Post SM, Abbas HA, Quintas-Cardama A, et al. The p53-Mdm2 feedback loop protects against DNA damage by inhibiting p53 activity but is dispensable for p53 stability, development, and longevity. Genes Dev. 2013; 27:1857–1867. [PubMed: 23973961]

14. Haupt Y, Maya R, Kazaz A, Oren M. Mdm2 promotes the rapid degradation of p53. Nature. 1997; 387:296–299. [PubMed: 9153395]

15. Honda R, Tanaka H, Yasuda H. Oncoprotein MDM2 is a ubiquitin ligase E3 for tumor suppressor p53. FEBS Lett. 1997; 420:25–27. [PubMed: 9450543]

16. McGowan KA, Li JZ, Park CY, Beaudry V, Tabor HK, Sabnis AJ, et al. Ribosomal mutations cause p53-mediated dark skin and pleiotropic effects. Nat Genet. 2008; 40:963–970. [PubMed: 18641651]

17. McGowan KA, Pang WW, Bhardwaj R, Perez MG, Pluvinage JV, Glader BE, et al. Reduced ribosomal protein gene dosage and p53 activation in low-risk myelodysplastic syndrome. Blood. 2011; 118:3622–3633. [PubMed: 21788341]

18. Terzian T, Dumble M, Arbab F, Thaller C, Donehower LA, Lozano G, et al. Rpl27a mutation in the sooty foot ataxia mouse phenocopies high p53 mouse models. J Pathol. 2011; 224:540–552. [PubMed: 21674502]

19. Itahana K, Mao H, Jin A, Itahana Y, Clegg HV, Lindstrom MS, et al. Targeted inactivation of Mdm2 RING finger E3 ubiquitin ligase activity in the mouse reveals mechanistic insights into p53 regulation. Cancer Cell. 2007; 12:355–366. [PubMed: 17936560]

20. Pant V, Lozano G. Dissecting the p53-Mdm2 feedback loop *in vivo*: uncoupling the role in p53 stability and activity. Oncotarget. 2014; 5:1149–1156. [PubMed: 24658419]

21. Liu G, Terzian T, Xiong S, Van Pelt CS, Audiffred A, Box NF, et al. The p53-Mdm2 network in progenitor cell expansion during mouse postnatal development. J Pathol. 2007; 213:360–368. [PubMed: 17893884]

Author Manuscript Author Manuscript Author Manuscript Author Manuscript

22. Zeron-Medina J, Wang X, Repapi E, Campbell MR, Su D, Castro-Giner F, et al. A polymorphic p53 response element in KIT ligand influences cancer risk and has undergone natural selection. Cell. 2013; 155:410–422. [PubMed: 24120139]
23. Vanover JC, Spry ML, Hamilton L, Wakamatsu K, Ito S, D'Orazio JA. Stem cell factor rescues tyrosinase expression and pigmentation in discreet anatomic locations in albino mice. Pigment Cell Melanoma Res. 2009; 22:827–838. [PubMed: 19682281]
24. Kunisada T, Yoshida H, Yamazaki H, Miyamoto A, Hemmi H, Nishimura E, et al. Transgene expression of steel factor in the basal layer of epidermis promotes survival, proliferation, differentiation and migration of melanocyte precursors. Development. 1998; 125:2915–2923. [PubMed: 9655813]
25. Okura M, Maeda H, Nishikawa S, Mizoguchi M. Effects of monoclonal anti-c-kit antibody (ACK2) on melanocytes in newborn mice. J Invest Dermatol. 1995; 105:322–328. [PubMed: 7545201]
26. Perry ME. The regulation of the p53-mediated stress response by MDM2 and MDM4. Cold Spring Harb Perspect Biol. 2010; 2:a000968. [PubMed: 20182601]
27. Steingrimsson E, Copeland NG, Jenkins NA. Mouse coat color mutations: from fancy mice to functional genomics. Dev Dyn. 2006; 235:2401–2411. [PubMed: 16691561]
28. Beumer TL, Roepers-Gajadien HL, Gademan IS, van Buul PP, Gil-Gomez G, Rutgers DH, et al. The role of the tumor suppressor p53 in spermatogenesis. Cell Death Differ. 1998; 5:669–677. [PubMed: 10200522]
29. Almon E, Goldfinger N, Kapon A, Schwartz D, Levine AJ, Rotter V. Testicular tissue-specific expression of the p53 suppressor gene. Dev Biol. 1993; 156:107–116. [PubMed: 7680625]
30. Sullivan JM, Jeffords LB, Lee CL, Rodrigues R, Ma Y, Kirsch DG. p21 protects 'Super p53' mice from the radiation-induced gastrointestinal syndrome. Radiat Res. 2012; 177:307–310. [PubMed: 22165824]
31. Post SM, Quintas-Cardama A, Pant V, Iwakuma T, Hamir A, Jackson JG, et al. A high-frequency regulatory polymorphism in the p53 pathway accelerates tumor development. Cancer Cell. 2010; 18:220–230. [PubMed: 20832750]
32. Jeffers JR, Parganas E, Lee Y, Yang C, Wang J, Brennan J, et al. Puma is an essential mediator of p53-dependent and -independent apoptotic pathways. Cancer Cell. 2003; 4:321–328. [PubMed: 14585359]
33. Jacks T, Remington L, Williams BO, Schmitt EM, Halachmi S, Bronson RT, et al. Tumor spectrum analysis in p53-mutant mice. Curr Biol. 1994; 4:1–7. [PubMed: 7922305]
34. Brugarolas J, Chandrasekaran C, Gordon JI, Beach D, Jacks T, Hannon GJ. Radiation-induced cell cycle arrest compromised by p21 deficiency. Nature. 1995; 377:552–557. [PubMed: 7566157]
35. Ventura A, Kirsch DG, McLaughlin ME, Tuveson DA, Grimm J, Lintault L, et al. Restoration of p53 function leads to tumour regression *in vivo*. Nature. 2007; 445:661–665. [PubMed: 17251932]
36. Marino S, Vooijs M, van Der Gulden H, Jonkers J, Berns A. Induction of medulloblastomas in p53-null mutant mice by somatic inactivation of Rb in the external granular layer cells of the cerebellum. Genes Dev. 2000; 14:994–1004. [PubMed: 10783170]
37. Shetty G, Wilson G, Huhtaniemi I, Boettger-Tong H, Meistrich ML. Testosterone inhibits spermatogonial differentiation in juvenile spermatogonial depletion mice. Endocrinology. 2001; 142:2789–2795. [PubMed: 11415997]

Author Manuscript
Author Manuscript
Author Manuscript
Author Manuscript

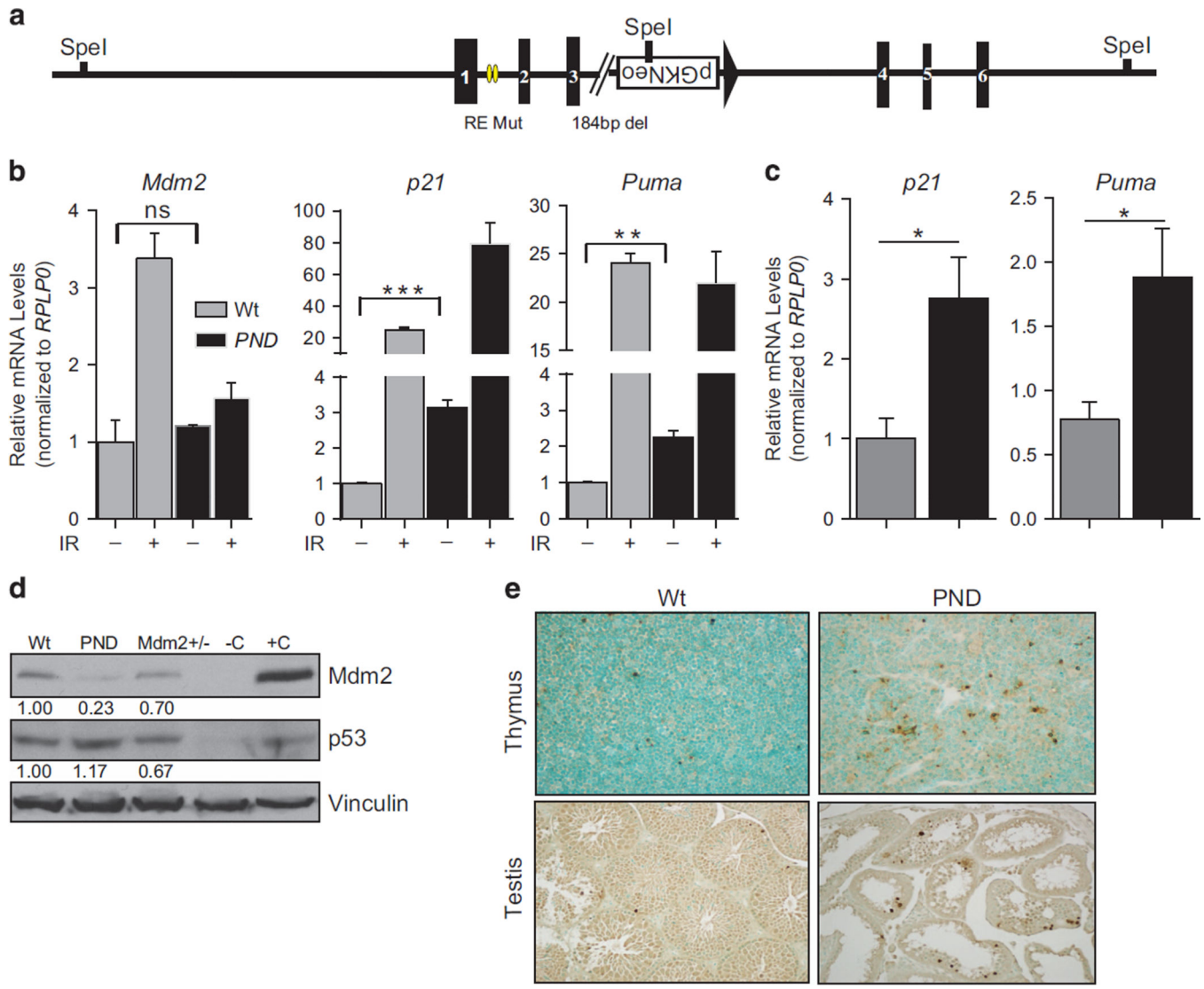

Figure 1.

Generation and characterization of the *Mdm2*$^{PND/PND}$ mice. (**a**) Schematic representation of the *Mdm2*^{PND} allele. Yellow ovals and broken line depict p53 response element mutations and a 184- bp deletion, respectively. (**b**) RT–qPCR for p53 targets in thymi of un-irradiated and irradiated *Mdm2*$^{PND/PND}$ mice. $n = 3$,±s.e.m., $*P < 0.05$, $**P < 0.01$, $***P < 0.001$. ns, non significant. (**c**) RT–qPCR for p53 targets in spleens of *Mdm2*$^{PND/PND}$ mice. $n = 3$, ±s.e.m., $*P < 0.05$. (**d**) Western blot from testis lysate of wild-type and *Mdm2*$^{PND/PND}$ mice. −C and +C represent negative and positive controls, respectively. (**e**) Representative TUNEL staining in thymus and testis of wild-type and *Mdm2*$^{PND/PND}$ mice.

Author Manuscript Author Manuscript Author Manuscript Author Manuscript

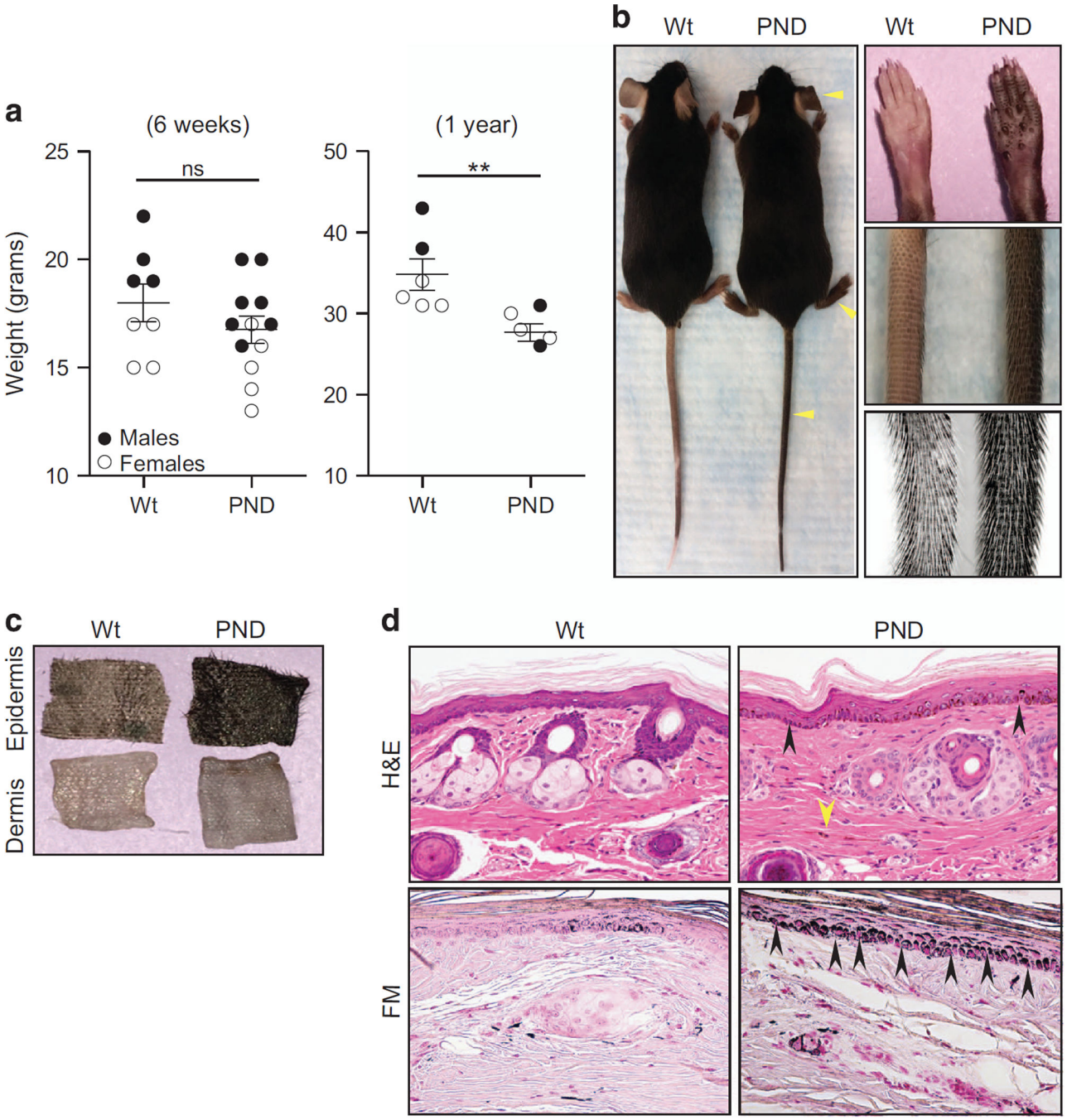

Figure 2.

Phenotypic aberrations in *Mdm2*$^{PND/PND}$ mice. (**a**) Comparative weights of age-matched wild-type and *Mdm2*$^{PND/PND}$ mice at 6 weeks (left) and 1 year of age (right). Filled and unfilled circles represent males and females, respectively.±s.e.m., $^{**}P < 0.01$. ns, non significant. (**b**) Hyperpigmentation in *Mdm2*$^{PND/PND}$ mice. Yellow arrowheads point to the extremities with noticeable differences from wild-type mice. Panel on the right shows close up of tail and paws from wild-type and *Mdm2*$^{PND/PND}$ mice. (**c**) Epidermal–dermal separation of wild-type and *Mdm2*$^{PND/PND}$ mouse skin. (**d**) Hematoxylin and eosin (H&E)-

Author Manuscript Author Manuscript Author Manuscript Author Manuscript

stained longitudinal section of mouse tail showing melanin accumulation (black arrows) and spindled melanocytes (yellow arrow) in *Mdm2*$^{PND/PND}$ mice (upper panel). Fontanna Masson (FM) stained tail sections from wild-type and *Mdm2*$^{PND/PND}$ mice marking melanin (lower panel).

Author Manuscript Author Manuscript Author Manuscript Author Manuscript

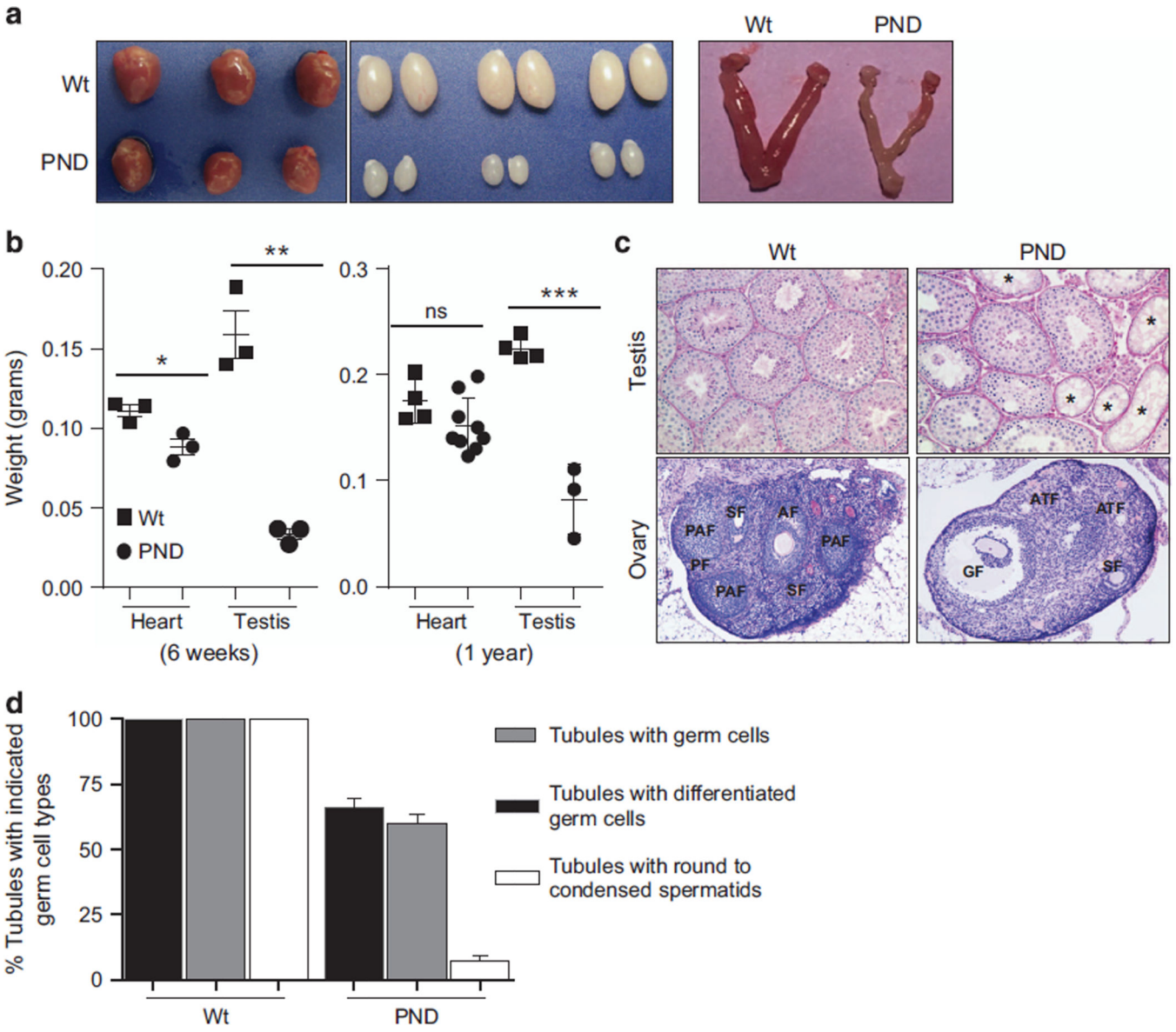

Figure 3.

Morphological differences in mouse tissues. (**a**) Representative images showing comparative size of heart, testis and uterine horns in wild-type and *Mdm2*$^{PND/PND}$ mice. (**b**) Comparative analysis of heart and testis weights from 6 weeks (left) and 1-year-old (right) wild-type and *Mdm2*$^{PND/PND}$ mice.±s.e.m., *$P < 0.05$, ** $P < 0.01$, ***$P < 0.001$. ns, non significant. (**c**) Representative periodic acid–Schiff (PAS)-hematoxylin-stained cross-sections of testis (20×) and hematoxylin and eosin (H&E)-stained sections of ovary (5×) from wild-type and *Mdm2*$^{PND/PND}$ mice. (**d**) Graphical representation of percentage of seminiferous tubule sections containing germ cells of different types in wild-type and *Mdm2*$^{PND/PND}$ mice testes. *Seminiferous tubules without germ cells; AF, antral follicle; ATF, atreal follicle; GF, Graffian follicle; PAF, preantral follicle; PF, primary follicle; SF, secondary follicle.

Author Manuscript Author Manuscript Author Manuscript Author Manuscript

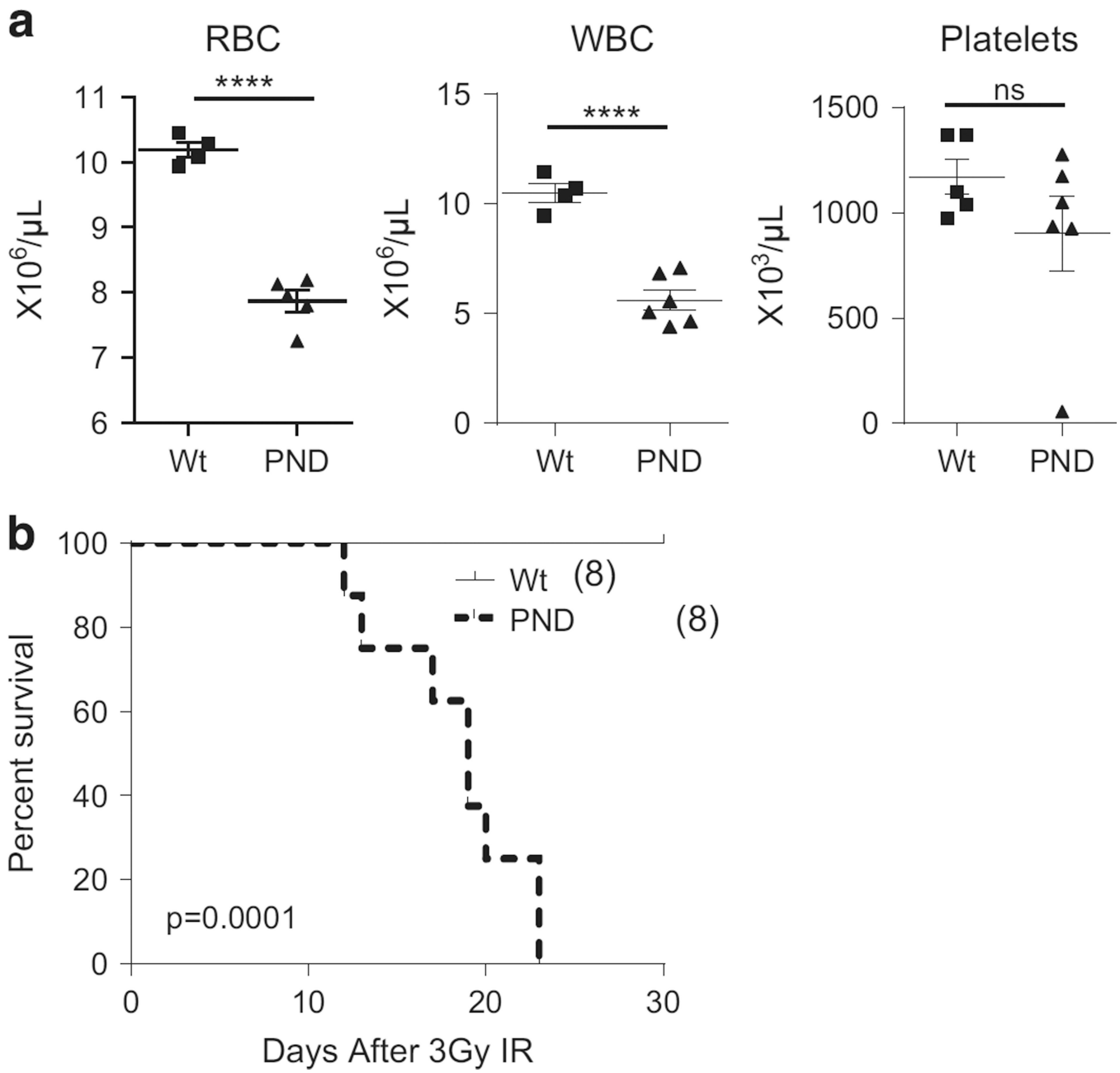

Figure 4.

Hematopoietic defects in *Mdm2*$^{PND/PND}$ mice. (**a**) Comparative red blood cell (RBC), white blood cell (WBC) and platelet counts from wild-type and *Mdm2*$^{PND/PND}$ mice. ±s.e.m., **** $P < 0.0001$. (**b**) Kaplan–Meier survival curve of wild-type and *Mdm2*$^{PND/PND}$ mice after 3 Gy IR.

Author Manuscript Author Manuscript Author Manuscript Author Manuscript

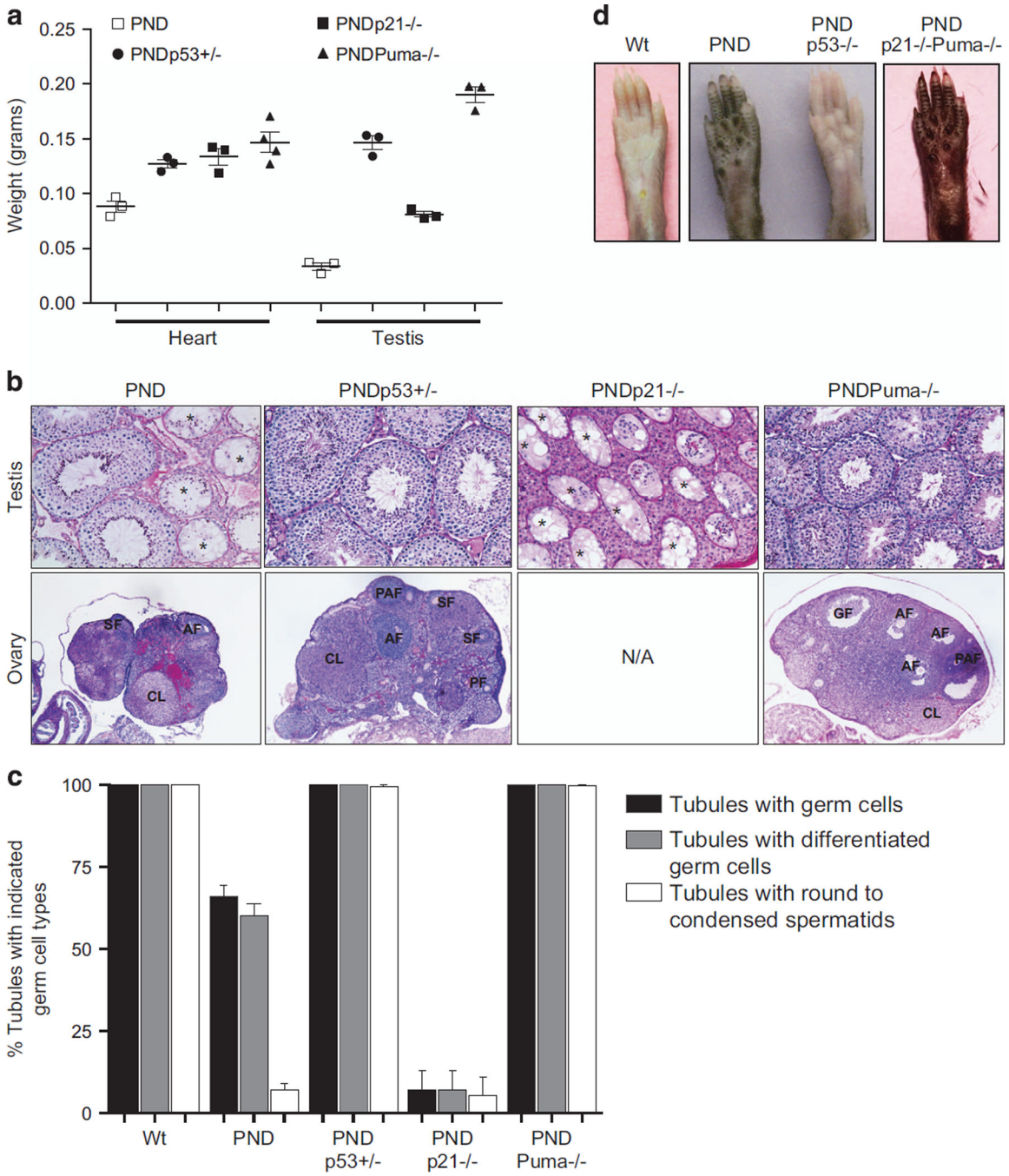

Figure 5.

Distinct targets manifest p53-dependent pathologies. (**a**) Comparative weights of hearts and testes from *Mdm2*$^{PND/PND}$, *Mdm2*$^{PND/PND}$ *p53*$^{+/-}$, *Mdm2*$^{PND/PND}$ *p21*$^{-/-}$ and *Mdm2*$^{PND/PND}$ *Puma*$^{-/-}$ mice. (**b**) Representative periodic acid–Schiff (PAS)-hematoxylin-stained testes (20×) and ovary (5×) cross-sections from *Mdm2*$^{PND/PND}$ *p53*$^{+/-}$, *Mdm2*$^{PND/PND}$ *p21*$^{-/-}$ and hematoxylin and eosin (H&E)-stained section from *Mdm2*$^{PND/PND}$ *Puma*$^{-/-}$ mice. (**c**) Graphical representation of percentage of seminiferous tubule sections containing germ cells of different types in *Mdm2*$^{PND/PND}$ *p53*$^{+/-}$,

Author Manuscript Author Manuscript Author Manuscript Author Manuscript

Mdm2$^{PND/PND}$ *p21*$^{-/-}$ and *Mdm2*$^{PND/PND}$ *Puma*$^{-/-}$ mice testes. (**d**) Representative picture showing changes in skin pigmentation in *Mdm2*$^{PND/PND}$ paws after deletion of p53 or after combined deletion of *p21* and *Puma*. *Seminiferous tubules without germ cells; AF, antral follicle; ATF, atreal follicle; CL, corpus luteum; GF, Graffian follicle; PAF, preantral follicle; PF, primary follicle; SF, secondary follicle.

Author Manuscript Author Manuscript Author Manuscript Author Manuscript

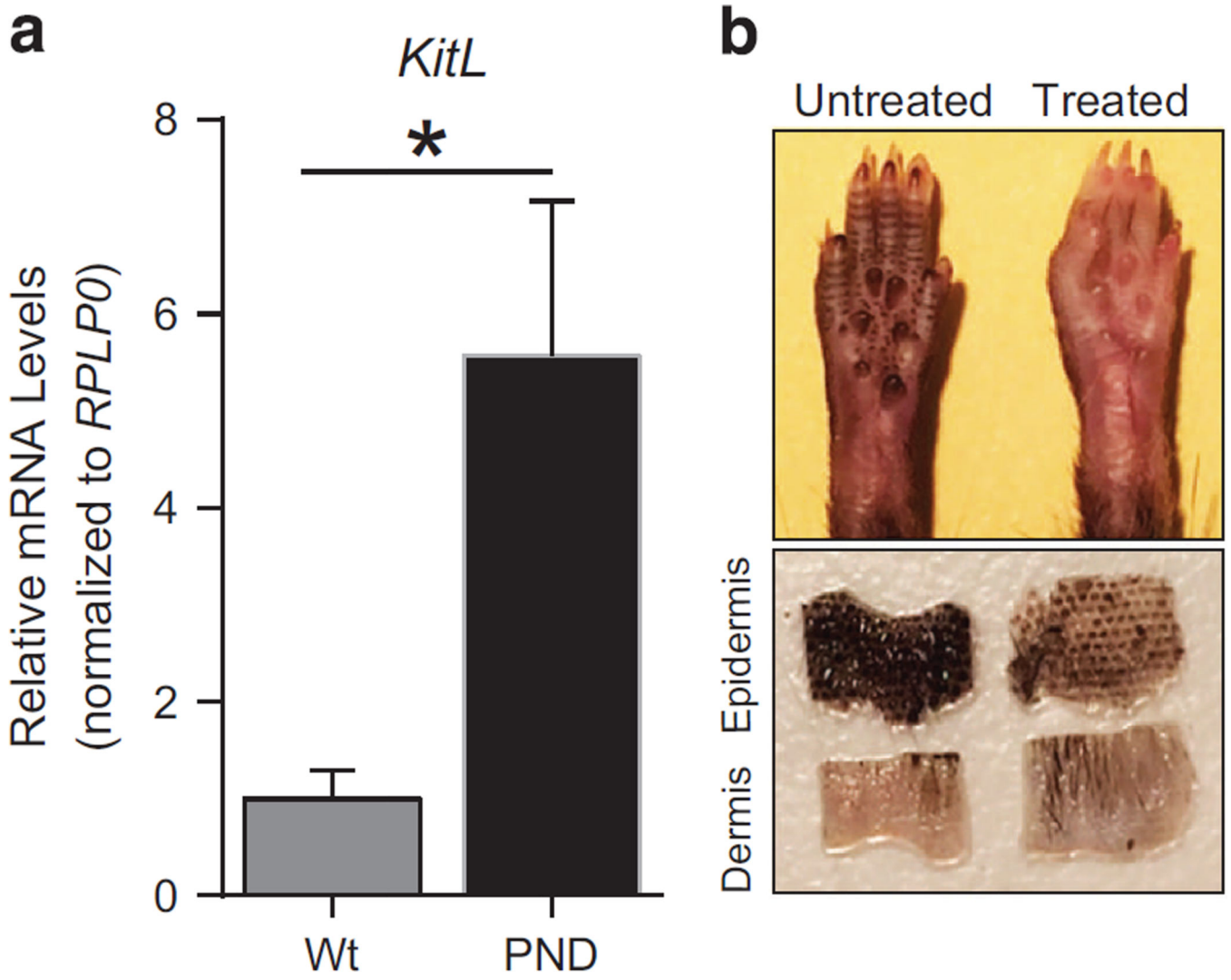

Figure 6.

Distinct targets manifest p53-dependent pathologies. (**a**) RT–qPCR for Kitl in keratinocytes of wild-type and *Mdm2*$^{PND/PND}$ mice. $n = 4$, ± s.e.m., $^{*}P < 0.05$. (**b**) Representative picture showing changes in skin pigmentation in *Mdm2*$^{PND/PND}$ *p53*$^{flox/flox}$*:CreERT2* mouse paws after tamoxifen injection (upper panel). Epidermal–dermal separation of untreated and tamoxifen treated *Mdm2*$^{PND/PND}$ *p53*$^{flox/flox}$*: CreERT2* mouse skin (lower panel).

Author Manuscript Author Manuscript Author Manuscript Author Manuscript

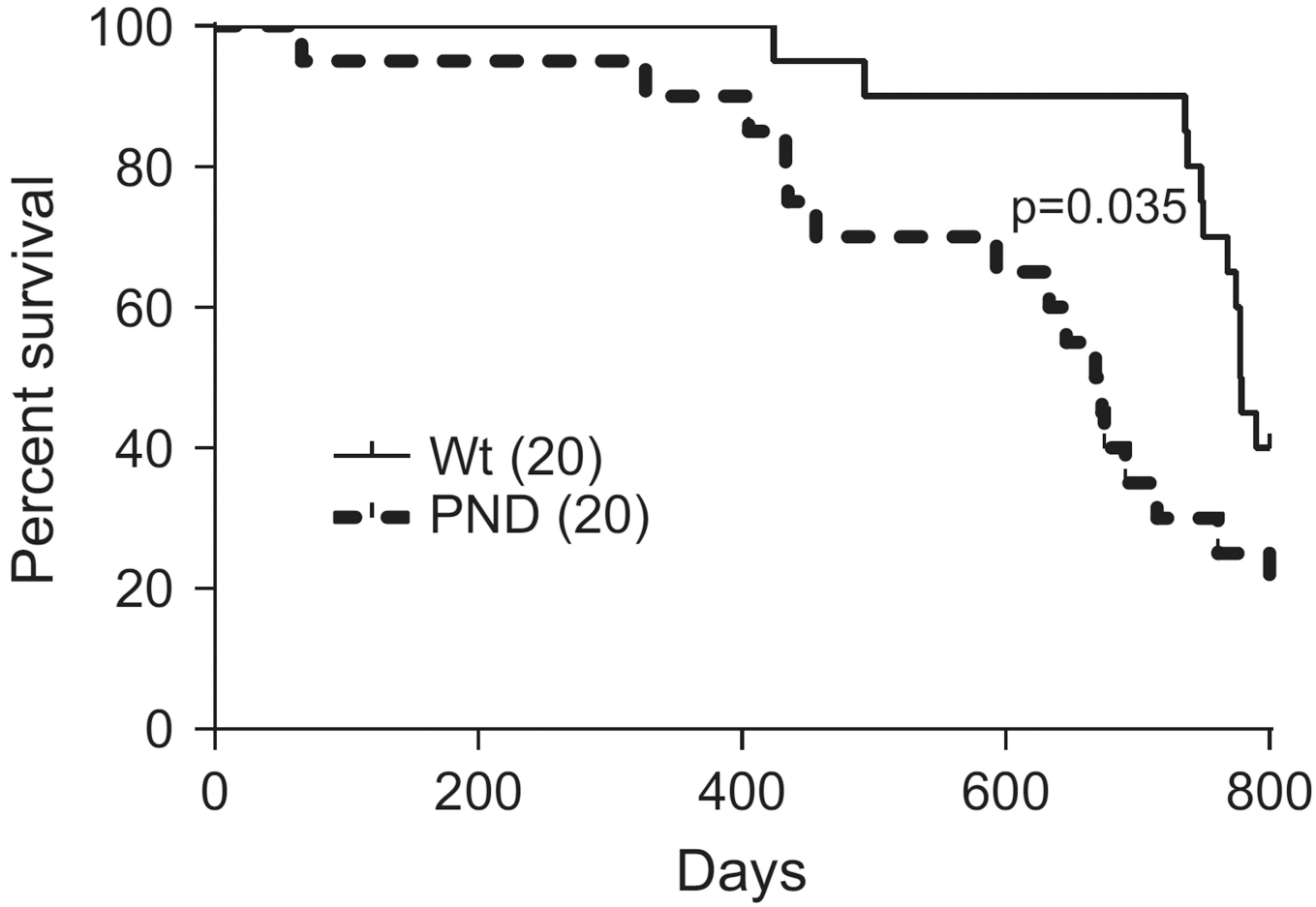

Figure 7.
Shortened life span in *Mdm2*$^{PND/PND}$ mice. Kaplan–Meier survival curve of wild-type and *Mdm2*$^{PND/PND}$ mice. Curves are censored at 800 days.